



**EYUP KOÇAK**

**ENERGY RECOVERY IN WATER SUPPLY SYSTEMS  
USING HYDROTURBINES**

**RECUPERAÇÃO DE ENERGIA EM SISTEMAS DE  
ABASTECIMENTO DE ÁGUA COM RECURSO A  
HIDROTURBINAS**



**EYUP KOÇAK**

**ENERGY RECOVERY IN WATER SUPPLY SYSTEMS  
USING HYDROTURBINES**

**RECUPERAÇÃO DE ENERGIA EM SISTEMAS DE  
ABASTECIMENTO DE ÁGUA COM RECURSO A  
HIDROTURBINAS**

Tese apresentada à Universidade de Aveiro para cumprimento dos requisitos necessários à aprovação da unidade curricular de Dissertação/Projeto/Estágio, realizada sob a orientação científica de António Gil d'Orey de Andrade Campos, Professor Auxiliar do Departamento de Engenharia Mecânica da Universidade de Aveiro

to my beautiful family...

## **o júri**

presidente

**Prof. Doutor Robertt Angelo Fontes Valente**  
professor associado da Universidade de Aveiro

**Prof. Doutor Vítor António Ferreira da Costa**  
professor catedrático da Universidade de Aveiro

**Prof. Doutor António Gil d'Orey de Andrade Campos**  
professor auxiliar da Universidade de Aveiro (orientador)

## **acknowledgments**

I owe my deepest gratitude to my visors Assoc. Prof. Dr. António Gil d'Orey de Andrade Campos and Prof. Dr. Nuri Yücel and their guidance, understanding and advice.

I would like to thank to Dr. Salih Karaaslan and Furkan Arundaş for their inspiration and guidance during my graduate education life.

I would like to thank to my flatmates in Portugal, Lennart, Sascha and Rebecca and flatmates in Turkey, Cahit and Hakan. They gave me encouragement and motivation whenever I needed. It was a great chance to share flats with them.

I would like to thank to everyone I had the pleasure to meet in ESN Aveiro, especially to the team responsible for the amazing events. Thank you, Teresa, Carolina, Diogo and all team!

I also owe thanks to friends from Erasmus Program, Inês, Memduh, İpek, Sanem, Carolina, Szymon, Joao, Class, Jakob, Seda, Sena and everyone who I met.

My deepest thanks to special friend, Merve who is making me stronger and happy.

I would like to thank to European Commission and Turkish National Agency for its financial support throughout this study.

Finally, I would like to thank my family for their endless support and love. Thank you for making my life better.

**keywords**

energy efficiency, energy recovery, water supply systems, micro hydroturbines

**abstract**

In the last century, the main source of hydroelectric power came from conventional dams and the energy produced by hydro turbines had a fast growing. New applications of turbines in hydro power even in micro-scale projects have emerged.

Water supply systems are large energy consumers due to the large amount of energy needed for pumping the water from low to high heights. However, gravity fed subsystems generally presents excess of pressure, which is lost with pressure reducing valves. Therefore, energy can be recovered from locals of excessively high flow and pressure. Nevertheless, water networks are highly complex systems and the flow conditions change instantaneously throughout the network. The control of the pressure is the top priority of the system providers and energy should be converted along with keeping the pressure to a desired level. The application of turbines appeared as an alternative to produce energy, to reduce leakage reductions and to manage network pressure.

This work aims to investigate the energy production in water supply systems using micro hydro turbines. To find the optimal location for the installation of micro hydro turbine in the network, a tool is developed using the hydraulic simulator EPANET for obtaining flow regimes of each pipe. Technical feasibility analysis is automatically computed for the selection of appropriate type turbine and the CFD program ANSYS is used to design and verify the hydraulic performance of the turbine. A financial analysis is performed and has showed that energy production in water supply systems using micro turbines is a profitable alternative and a renewable solution for the world's growing energy needs.

**palavras-chave**

Eficiência energética, recuperação de energia, sistemas de abastecimento de água, microturbinas hidráulicas

**resumo**

No século passado, a principal fonte de energia hidroelétrica provinha de barragens convencionais e a energia produzida pelas turbinas hidráulicas teve um crescimento rápido. Neste século, novas aplicações de turbinas geradoras de energia elétrica, mesmo em projetos de microescala, emergiram. Os sistemas de abastecimento de água são grandes consumidores de energia devido à grande quantidade de energia necessária para o bombeamento de água de baixas para elevadas alturas manométricas. No entanto, os subsistemas alimentados graviticamente apresentam geralmente excesso de pressão, que se perde com válvulas de redução de pressão. Portanto, a energia pode ser recuperada de locais de caudal e pressão excessivamente elevados. No entanto, as redes de água são sistemas altamente complexos cujas condições hidráulicas mudam instantaneamente em toda a rede. O controle da pressão é a principal prioridade dos fornecedores e a energia deve ser recuperada ao mesmo tempo que se mantém a pressão desejada. A aplicação de turbinas aparece como uma alternativa para produzir energia, reduzir fugas e gerir a pressão da rede. Este trabalho tem como objetivo investigar a produção de energia em sistemas de abastecimento de água usando microturbinas hidráulicas. Para encontrar a localização ideal para a instalação da microturbina hidráulicas na rede, desenvolve-se uma ferramenta que recorre ao simulador hidráulico EPANET para obter regimes de escoamento de cada conduta. A análise de viabilidade técnica é calculada automaticamente para a seleção da turbina adequada e o programa CFD ANSYS é usado para projetar e verificar o desempenho hidráulico da turbina. Uma análise financeira é realizada e mostra que a produção de energia em sistemas de abastecimento de água usando microturbinas é uma alternativa lucrativa e uma solução renovável para as crescentes necessidades energéticas do mundo.

## Contents

List of Figures .....	1
List of Tables .....	3
Nomenclature.....	4
1. Introduction.....	7
2. Energy Production in Water Supply Systems .....	10
3. Methodology .....	14
3.1 The Selection of Most Adequate Site for a Turbine Installation.....	15
3.2 Determination of Turbine or PATs Characteristics .....	15
3.3 Turbine CFD Analysis .....	17
4. Numerical Studies and Case Study .....	23
4.1 The Napoli East Network.....	23
4.2 Technical Feasibility Results .....	26
4.3 Pump Design and CFD Validation.....	27
4.4 PAT CFD Analysis .....	33
5. Financial Analysis.....	37
6. Conclusions, Contributions and Recommendations .....	39
7. References.....	42



## List of Figures

Figure 1. Flowchart of the general methodology of the present study.....	14
Figure 2. Relationship between $K$ and $E_{recov}$ .....	16
Figure 3. General design methodology of the turbo machinery components .....	19
Figure 4. Effect of specific speed on the impeller geometry (Yedidiah, 1996) .....	20
Figure 5. Velocity triangle drawn (a) for the inlet and (b) for the outlet .....	20
Figure 6. The basic dimensions of runner meridional channel .....	20
Figure 7. (a) Elevation map of the study area and (b) layout of Napoli Est water distribution system and locations of three scenarios. The Napoli Est water distribution system serves an area of approximately 920 hectares, covering most of the eastern zone of the city. The number of inhabitants is around 65,000-70,000 and the elevation ranges between 11-78 m above a sea level (Fontana et al., 2012).....	23
Figure 8. The flow duration curves of pipe 1 (a) before and (b) after the PRV implementation.....	25
Figure 9. (a) Dimensions of preliminary pump runner meridional channel and (b) meridional profile by ANSYS Bladegen 16.1 .....	28
Figure 10. 3-D Illustration of the preliminary runner design.....	29
Figure 11. Full turbine geometry .....	30
Figure 12 Single Blade Analysis Relative Velocity Streamlines (a)Preliminary Design (b)Final Design .....	31
Figure 13 Single Blade Analysis Meridional Profile Pressure Distributions (a) Preliminary Design (b) Improved Design (c) Final Design.....	31
Figure 14 Single Blade Analysis Absolute Pressure Distributions and Cavitation Control (a) Preliminary Design (b) Final Design .....	32
Figure 15. Full pump analysis results at 1450 rpm .....	32
Figure 16. Results of the final design (a) total pressure contours of the full pump and (b) pressure contour of the meridional plane of the runner.....	33
Figure 17. Flow duration curves of pipes (a) P151 and (b) P198 after the PRV implementation .....	34
Figure 18. Comparison of the CFD result with the estimation curve (see Equation 11 and 12).....	35

Figure 19. Turbine installation efficiency curves for (a) Scenario B3, where Kaplan Turbines were applied (Obtained by Equation 16 and 17), and for (b) Scenario B2, where particular designed PATs where applied..... 36

## List of Tables

Table 1. Operation range for the main existent hydro turbines in terms of head (European Small Hydropower Association, 2004b). .....	17
Table 2. Results for the Napoli Est network (scenarios, A to C). Comparison with scenarios, S3, S6, S8 (Coelho and Andrade-Campos, 2017) and A <sub>F</sub> , B <sub>F</sub> , D <sub>F</sub> (Fontana et al, 2012).....	24
Table 3. Technical pre-analysis results of daily net energy production for each scenario. The results of Coelho and Andrade-Campos (2017) are also presented for comparison purposes .....	27
Table 4. Boundary conditions of the full geometry .....	29
Table 5. Optimization design parameters .....	30
Table 6. Numerical results of the PAT and comparison with the estimated head and power values that are obtained from Equation 11 and 12. ....	36
Table 7. Annual income and investment costs.....	37
Table 8. Preliminary income analysis .....	38

## Nomenclature

$b_2$	=	gate head	(m)
$C$	=	absolute velocity	(m s <sup>-1</sup> )
$C_{1m}, C_{2m}$	=	vertical component of absolute velocity vector	(m s <sup>-1</sup> )
$C_{1u}, C_{2u}$	=	horizontal component of absolute velocity vector	(m s <sup>-1</sup> )
$C_{\varepsilon 1}, C_{\varepsilon 2}$	=	constants	(-)
$D$	=	link diameter	(m)
$D_1$	=	inlet diameter of runner	(m)
$D_2$	=	outlet diameter of runner	(m)
$d_s$	=	shaft diameter	(m)
$E_{\text{recov}}$	=	recovered energy	(J)
$g$	=	gravitational acceleration	(m s <sup>-2</sup> )
$H$	=	head	(m)
$H_d$	=	design head	(m)
$h$	=	minor head losses	(m)
$K$	=	minor loss coefficient	(-)
$n$	=	rotational speed	(rpm)
$n_s$	=	dimensionless specific speed	(-)
$n_{\text{dnodes}}$	=	number of demand nodes	(-)
$p'$	=	modified pressure	(Pa)
$P$	=	pressure	(Pa)

$P_{\min}$	=	minimum pressure in demand nodes	(Pa)
$W_{\text{net}}$	=	net power	(W)
$PRV$	=	pressure reducing valve	(-)
$S_m$	=	sum of forces	(N)
$t_{\text{step}}$	=	duration of the time step	(s)
$Q$	=	flow rate	( $\text{m}^3 \text{s}^{-1}$ )
$Q_d$	=	design flow	( $\text{m}^3 \text{s}^{-1}$ )
$Q_{\text{peak}}$	=	turbine peak efficiency flow	( $\text{m}^3 \text{s}^{-1}$ )
$Q_t$	=	turbine rated flow	( $\text{m}^3 \text{s}^{-1}$ )
$U$	=	impeller velocity	( $\text{m s}^{-1}$ )
$W$	=	relative velocity	( $\text{m s}^{-1}$ )
$WSS$	=	water supply system	(-)
$\beta_1$	=	leading edge lean angle	( $^\circ$ )
$\beta_2$	=	trailing edge lean angle	( $^\circ$ )
$\eta_{F,\text{above}}$	=	Francis turbine efficiency for flows above $Q_{\text{peak}}$	(-)
$\eta_{F,\text{under}}$	=	Francis turbine efficiency for flows under $Q_{\text{peak}}$	(-)
$\eta_{F,\text{peak}}$	=	Francis turbine peak efficiency	(-)
$\eta_{K,\text{peak}}$	=	Kaplan turbine peak efficiency	(-)
$\eta_K$	=	Kaplan turbine efficiency	(-)
$\eta_t$	=	turbine efficiency	(-)
$\rho$	=	fluid density	( $\text{kg m}^{-3}$ )

$\mu_{\text{eff}}$  = effective viscosity (Pa s)

$\mu_t$  = turbulence viscosity (Pa s)

$\sigma_k, \sigma_E$  = constants (-)

## 1. Introduction

During the last years, researchers have investigated strategies of energy efficiency in water supply systems (WSSs). The strategies of energy efficiency in WSSs can pass through simple monitoring operations for leakages control to more complex operations such as the water demand prediction, pump systems optimization, storage/production reservoir systems optimization and real-time operations (Coelho-Andrade-Campos, 2014). Almost all techniques aim two purposes; (i) both energy saving and (ii) water leakage reduction. One of the important part of waters leakage management is pressure management. Pressure can be reduced to limit leakage, however operational conditions should be guaranteed through adequate pressure head over the network. A common way to reduce pressure is to impose flow or pressure reducing valves (PRV) in water networks.

Other possibility to save energy in WSSs is through energy recovery. Ramos et al. (2011) and Perez-Sanchez et al. (2017) indicated that energy saving and recovery using turbines is a very attractive possibility in WSS due to the small additional costs required. In hydropower systems, it is usual the use of turbines or pumps operating as turbines (PATs) for the recovery of the excess of energy that is generally lost in the WSS due to the use of pressure reduction valves. Such turbo machines extract the potential energy from the fluid (water) and convert it into useful work. However, the selection of the most adequate and profitable site in a network for the installation of a certain type of turbine is generally not a simple task due to the complexity of the network and the variability of the conditions (Coelho, 2016). Additionally, each hydropower project requires a different turbine design.

The analytical design of turbines is generally not a simple task due to the complexity of the blade shape and the variability of the conditions for hydropower generation. However, the modelling of the turbine and its operational verifications are costly and time consuming. Nevertheless, these tests are essential to evaluate the design. For this reason, nowadays, researchers prefer computational fluid dynamics (CFD) design methods. CFD-based design methods allow observing all flow characteristics (particle speed, pressure, cavitation, hydraulic efficiency, etc.) without requiring previous manufacturing

process, which is not always possible with conventional measuring instruments and it is much cheaper than experimental testing.

This work focuses on energy production using micro hydro turbines in any water supply systems and it consists of three parts. In the first part, a methodology is determined for both the identification of sites and the selection of the adequate type turbines. A computational tool is developed for the case study. After presenting the initial results obtained from the tool, scenarios are created and technical feasibility analysis is performed. The first part provides the location for the maximization of energy in water supply systems.

In the second part, a pump as turbine (PAT) performance analysis with a computational fluid dynamic methods (CFD) is presented in terms of both pump and turbine operation. The pump design is obtained through a turbomachinery design tool, which resulted from the empirical and theoretical equations. CFD results are obtained and optimization studies are carried out in order to reach higher hydraulic efficiency. The main aim of the second part is to observe the performance of PAT to produce energy, installed into the predetermined location by tool. The effects of site conditions, variability of head and flow rate values, and comparisons with different type of turbines are investigated using CFD simulation.

In the third part, a financial feasibility analysis is conducted to determine the most attractive and profitable scenario. Results obtained in the first and second parts are used as a input data.

The outline of the work is as follows:

- In Chapter 2, the state-of-art is given briefly and previous studies are summarized. WSS investigation studies, pressure management and energy production in WSSs, turbo machinery design methodologies, CFD based turbomachinery application studies are selected as reference studies.
- In Chapter 3, the methodologies used throughout this dissertation are defined in order to achieve the main objectives.
- In Chapter 4, the selected case study is analyzed for the implementation of pressure reduction valves and distinct type turbines. After preliminary technical analysis of the scenarios, one of



the created scenario is selected for the CFD analysis. ANSYS 16.1 is used to design and verify the hydraulic performance of the turbine.

- In Chapter 5, financial analyses of the scenarios are performed to obtain all costs and profits for the case study.
- In Chapter 6, the study is summarized. Conclusions, contributions to the literature and recommendations for the future studies are also presented.

## 2. Energy Production in Water Supply Systems

Water distribution systems are rather complex systems and researchers are focused on how to reduce water losses and provide a top-quality service while operating efficiently (Giugni et al 2014). In recent years, linear, non-linear, dynamic programming or similar techniques were used to solve engineering problems with complex networks and reservoir systems. To use optimization techniques that can guarantee global optimal solutions, simplifications of physical systems are often used, particularly mathematical models. Various problem-specific assumptions are used to represent the system in a mathematical form that can be conveniently handled by an optimization tool. An exhaustive representation of the physical system along with a mathematical modelling technique that provides near-optimal solutions can be accepted for most of the real-life problems (Teegavarapu and Simonovic, 2002). Investigators have developed numerical methods using these techniques or have used specific software (e.g., EPANET and WaterGEMS), which are able to analyze the behavior of WSSs. Often, these models are used for the selection of profitable site for energy production or reducing water losses in a water supply network. Teegavarapu and Simonovic (2002) developed a mixed integer nonlinear programming (MINLP) method and compared with a simulated annealing (SA) technique in order to obtain the optimal power generation values at each of the hydropower plants. Both of techniques have been applied to a system of four hydropower generating reservoirs in Manitoba, Canada. The MINLP and SA models were run for similar conditions. Results showed that the SA model provided a better value of the objective function than the MINLP model. Corcoran et al. (2015) compared a nonlinear programming (NLP) to a mixed integer nonlinear programming approach and to an evolutionary optimization approach to find the optimal locations to install turbines for maximizing power generation in a WSN. The first part of their study involves comparing these approaches at a theoretical five-node network. The results showed that the mixed integer nonlinear programming approach was the most suitable technique. Authors then applied NLP and MINLP techniques at a 25-node network to find optimal locations for turbine installation. For small networks, the NPL model results were very consistent and its relative errors ranged between  $-0.036\%$  and  $+0.003\%$ . On the other hand, for a large-scale network, the MINLP approach provided very accurate approximations of the flow rates and

pressures in the network, with the largest relative error in a link reported as 1.96%. The results of their studies show that optimization algorithms can be used as a decision support tool in the design process of hydropower turbines installation in water supply networks (Corcoran et al. 2015).

Ramos et al. (2010) studied numerical and experimentally the behavior of pressure reducing valves and pump as turbines (PAT) in water distribution system. Experimental analyses have shown an equivalent behavior between PAT and PRV for general normal operating conditions. Financial analysis showed that the hydro-machine cost pay-back is obtained in about three years and the total payback time is around nine years. Another study of Ramos et al. (2011) discusses three different methods to evaluate energy recovery or reducing operational costs. The results showed that using a water turbine to convert the excess energy in the gravity pipe branches is an acceptable method for energy recovery. If the same amount of energy had been produced by burning coal/gas, nine times more equivalent CO<sub>2</sub> would have been emitted to the atmosphere. The second method showed that the optimization of the pumping operational schedules does not affect the electricity consumption or the air pollution but reduces considerably the operational cost. In the third method, a wind turbine is included in the system to provide power to the water pump. For this case, less electricity from the grid is consumed and the CO<sub>2</sub> emissions are reduced by at least half of the normal operation mode.

The optimal design of a turbine should take into account both technical parameters, such as the specific speed, diameter and efficiency of the turbine, and financial parameters, such as the costs of equipment and installation, including costs for civil works (Coelho, 2016). The turbomachinery design is not a simple task because the components depends on the turbine type and characteristics. All hydraulic machines have two particular components that, although the design objective is identical, require different design methodology: runner and vanes. For all turbo machineries, the most critical component is the runner that is composed of blades which have complex geometries and transfer energy from the fluid to the shaft. In the 20th century, researchers developed several methodologies which were specific speed dependent. Several of these methodologies are empirical and were found through experimental studies used to understand the fluid behavior inside the turbine.

Petermann (1964) developed analytical methodologies which are based on experimental studies for each kind of turbomachine such as pump, Francis, Kaplan, Pelton, gas turbine, steam turbine and turbine components. For hydro machines, methodologies were based on both specific speed and infinite blade theorem. Petermann also presented drawing methods for turbine components and their manufacturing process. Another important design approach of turbines is the Bovet method (Bovet, 1963) which uses empirical equations to obtain the parameters of the Francis hydro turbine runner. The Bovet methodology, that uses the dimensionless specific speed as reference, allows to compute the geometry of the hub and shroud (the generating curves) in the runner's blade zone. The streamlines angles can also be calculated using Bovet method (Miloş and Bărglăzan, 2004; Bovet, 1963). McBride (1979) deals with the turbomachinery design and analysis of turbomachinery in an incompressible, steady flow. Equations of motion are developed in order to model the blade row span wise and chord wise loading distributions on a blade row and to determine their effect on the through-flow.

Nowadays, more efficient turbo machines can be designed using numerical methodologies and computational tools. Acharya et al. (2015) optimized a cross-flow turbine using CFD methods. They have chosen a base design of turbine and investigated the effect of the nozzle shape, guide vane angle and the blade number in a runner. Efficiency of the cross-flow turbine was improved from 63.67% to 76.70% due to optimization studies. Deyou et al. (2015) investigated hump characteristics of a pump turbine model. Unsteady incompressible turbulent flow simulations were performed for the full pump turbine model using ANSYS ICEM 14.0 and the results were compared with experimental data. During the numerical simulation, four different mass flow values were determined as operation points in the hump region. Results showed that the vortex generation occurred in tandem cascade and the strength and range of the vortex groups changed with different discharges. Anup et al (2014) conducted a numerical study and validation in a Francis turbine by using a  $k\omega$ -based *SST* turbulence model. Transient analysis showed that periodical pressure and torque behaviors occurred all around the runner and all the guide vanes. The authors also comment as an important phenomenon the pressure fluctuation due to rotor-stator interaction and the occurrence of vortex rope in draft tube. That phenomena were investigated numerically at partial load operation condition.

Choi et al. (2013) studied rehabilitation of a Francis turbine runner by changing internal parameters of the runner while using the old turbine components such as spiral case, guide vanes and spiral casing. The CFD-based optimization studies of the runner and different guide vane operating conditions were also validated experimentally. Experimental tests showed that the total efficiency of the turbine was increased about 9.93%.

Another similar 500-kW Francis turbine performance improvement study was carried out by Teran et al. (2016). Part by part optimization techniques, which are based on Artificial Neural Networks (ANN) and Genetic Algorithms (GA) were implemented in their study. According to their numerical results, the turbine hydraulic efficiency was increased in 14.77% and the structural effects were minimized. Wang et al. (2017) redesigned a blade geometry for PATs using theoretical calculations for reverse operating conditions and the new design was analyzed numerically and experimentally. ANSYS CFX was used to analyze the flow through a PAT impeller with forward curve blades. Experimental studies of Wang et al. (2017) showed that the best efficiencies on reverse mode of pump increased when the original impellers were replaced with the special impellers.

As seen in previous studies, the CFD-based methodologies and optimization techniques make possible to efficiently design hydraulic machines and allows to observe the fluid flow behavior throughout turbine components.

### 3. Methodology

The methodology applied in this work can be divided into three main stages: (i) determination of potential sites for energy recovery, (ii) selection of an appropriate type of micro turbine, design and CFD analysis of selected turbine and (iii) preliminary financial analysis.

The water networks are very complex systems and the obtention of the flow characteristics in daily operation is not a simple task. Consequently, computational programs can be efficient tools for the analysis of the water networks and determination of potential turbine installation location. In this study, the fluid behavior in each pipe of the network is analyzed through a hydraulic simulator, particularly the EPANET 2.0 (EPANET, 2017). The main purpose of this analysis is to create scenarios of maximum recovered power from the network. The second stage of this study comprehends the design of the selected type turbine and the CFD-analysis of its hydraulic performance. According to the studies in Chapter 2, the use of pump as turbine instead of traditional turbine is an alternative solution for producing energy. Pump design, optimization processes and normal/reverse mode CFD analysis are carried out to obtain data for the third stage. In the third stage, a preliminary financial analysis based on the literature models is used to determine projects suitability for investment. These 3 stages are presented in Figure 1.

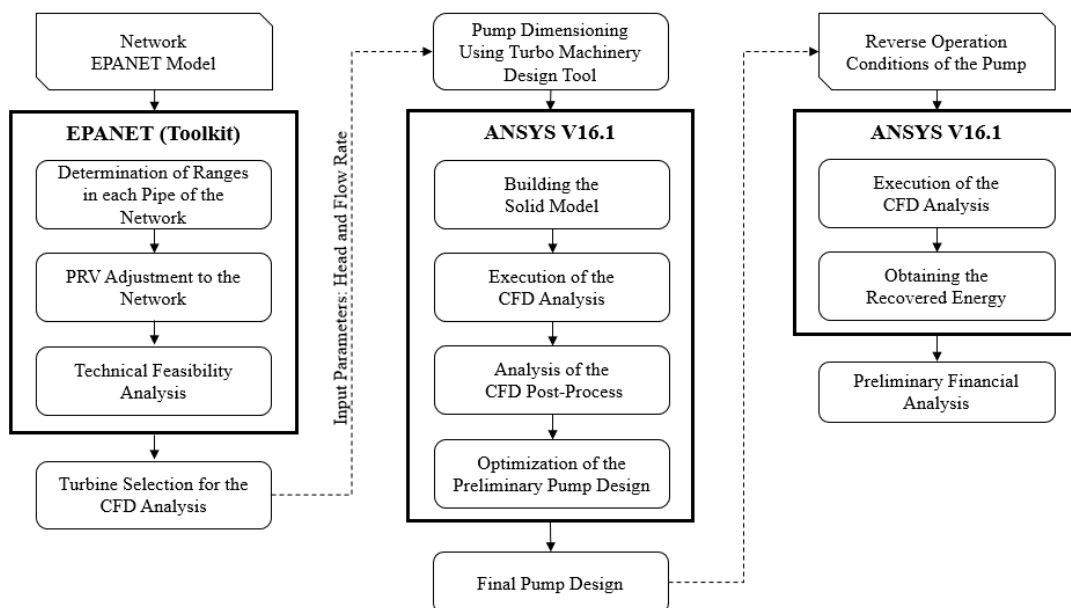


Figure 1. Flowchart of the general methodology of the present study

### 3.1 The Selection of Most Adequate Site for a Turbine Installation

In water supply systems, conducts can be found with different flow characteristics such as flow rate and pressure value, and placed in different locations and altitudes. Flow rates and pressure values in each location can be variable in time due to the variation of water levels in reservoirs and water demand by inhabitants. Due to the hourly variability of flow rates and head drop, the detailed analysis of WSS should be done for the selection of the adequate site. In order to determine the design flow in potential sites, the representation of flow-duration curves (FDC) is a common practice (Coelho 2016; European Small Hydropower Association, 2004a; Natural Resources Canada, 2005). This type of representation provides, for each recorded value of mean daily flow, the percentage of time that such value is equaled or exceeded, i.e. provides the number of days that presented the same value of mean flow during the period of recorded data (Coelho, 2016).

After determining the design flow and using the design head for a specific site, the net recoverable power can be calculated with the following equation:

$$W_{\text{net}} = \rho g H_d Q_d \eta_t, \quad (1)$$

where  $Q_d$  is the design flow ( $\text{m}^3/\text{s}$ ),  $H_d$  is the design head (m),  $\rho$  is the fluid density ( $\text{kg}/\text{m}^3$ ),  $g$  is the gravitational acceleration ( $\text{m}/\text{s}^2$ ) and  $\eta_t$  is the efficiency of turbine/PAT. The most adequate site for a turbine installation would be the site that presents the maximum net recoverable power. However, pressure conditions should be respected.

### 3.2 Determination of Turbine or PATs Characteristics

Generally, turbines are acted by water, which changes pressure as it moves through the turbine runner and transfer the energy to a runner shaft. Conventional turbine applications aim to absorb all pressure before the fluid reach the outlet of the turbine. But in water supply systems, minimum pressure level should be maintained for the whole network even while turbine operation. The model of a pressure reduction valve in water supply systems allows to analyze flow characteristics on selected link and able to verify the pressure management. The head drop through a PRV can be computed by the equation of the minor head losses through the link, that can be written as:

$$h = K \frac{8}{\pi^2 g} \left( \frac{Q}{D^2} \right)^2, \quad (2)$$

where  $D$  is the link diameter (m),  $Q$  is the flow rate ( $\text{m}^3/\text{s}$ ) and  $K$  is the resistance coefficient (Coelho, 2016). In this work, the determination of optimal locations for a turbine installation is performed using an optimization approach that consider the maximum dissipated energy using PRVs. The optimization approach can be formulated as:

$$\begin{aligned} &\text{maximize} && E_{\text{recov}} = \rho g \sum_t Q_t h(K) t_{\text{step}}, && t = 1, \dots, n_{\text{steps}} && (3) \\ &K && && && \end{aligned}$$

$$\begin{aligned} &\text{subject to} && P_{i,t} - P_{\text{min}} \geq 0, && i = 1, \dots, n_{\text{dnodes}} && (4) \end{aligned}$$

where  $E_{\text{recov}}$  is the recovered energy (J),  $t_{\text{step}}$  is the duration of the time-step,  $n_{\text{dnodes}}$  is the number of demand nodes,  $P_{\text{min}}$  is the minimum pressure required in the demand nodes (m) and  $P$  is the pressure at node  $i$  in the time-step  $t$ .

The solution of Equation 3 and 4 is used to obtain scenarios in a network modelled with EPANET toolkit and to determine the valve's maximum minor loss coefficient that maximizes the potentially recoverable energy.

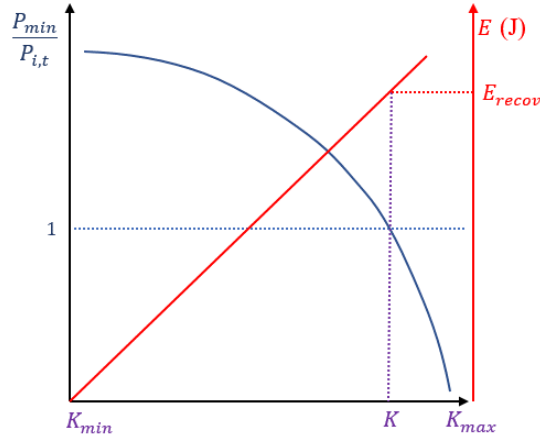


Figure 2. Relationship between  $K$  and  $E_{\text{recov}}$

A bisection method can be used to solve the presented optimization problem. In the first iteration,  $K_{\text{min}}$  and  $K_{\text{max}}$  can be determined as a minimum and maximum values and the process starts to assign a minor loss coefficient  $K$  to pipe. The new assigned minor loss coefficient is increased or decreased iteratively



by half size of interval between new and old  $K$  values until Equation 4 is satisfied. When Equation 4 reaches zero, the iterative process stops and maximum  $E_{\text{recov}}$  is obtained.

The determination of the average daily head drop and flow rate allows to select the turbine type via operation range charts or calculation techniques which are based on experimental studies. According to European Small Hydropower Association (2004b), the head range should be the first criterion to take into account in the turbine's selection. Table 1 shows the operation head ranges for each type of turbine, considering the five available types of hydraulic turbines (Francis, Kaplan, Pelton, Turgo, Crossflow) used in WSSs. However, some works obtained quite good results using PATs instead of turbine installation (Pateis et al. 2016; Carravetta et al. 2012; Fecarotta et al. 2011; Giugni et al. 2013 ; Fontana et al. 2012). In the last years, the use of PAT is suggested for energy production due to the low installed power and the need to reduce both the activation and maintenance costs (Pateis et al, 2016).

Table 1. Operation range for the main existent hydro turbines in terms of head (European Small Hydropower Association, 2004b).

Operation Range	Turbine Type	
50<H<1300	Pelton	impulse
50<H<250	Turgo	impulse
10<H<350	Francis	reaction
3<H<250	Cross-Flow	impulse
2<H<40	Kaplan/propeller	reaction

### 3.3 Turbine CFD Analysis

Turbo machines are categorized according to the type of flow, the type of blade rotation and the energy absorber or producer such as turbines and pumps. Each kind of turbine contains different components (blade, vane, spiral case, draft tube, nozzle, bucket, wicket gate, etc.). The design of all these components is costly and takes considerable time due to the efficiency tests. Flow separations on boundary layers, vortex generation, cavitation, erosion wear, vibration due to unbalanced pressure distributions are the main problems, which affect negatively both the hydraulic efficiency and useful/service life of the equipment. The development and interaction of boundary layers cannot be

completely analyzed theoretically. To predict the behavior of fluids in turbulent flow, numerical calculations based on turbulent models can provide better solutions. In general, the peak efficiencies of turbines developed with modern design tools like CFD-based tools have enabled to achieve the range of 70% to almost 96% (Liu et al. 2015).

Generally, CFD-based design methodologies are iterative processes and start with a preliminary design that is found using analytical methods. The design methodology used in this work is shown in the flowchart of Figure 3. For all turbo machines, the preliminary design is based on the net head and flow rate in the system. Recently, researchers use the developed tools for determining initial conditions and preliminary design of turbine components. These tools include some empirical and theoretical formulas. The necessary information for the CAD models is obtained from design tools and the preliminary solid model is subject to a CFD solver for the evaluation of the hydraulic performance of each component. After the evaluation of CFD results, the optimization loop takes places between solid model design parameters and CFD simulation post-process. The first step in the response surface optimization scheme is to define the goals of the optimization such as angles on blade, dimensions of meridional canal, spiral case sections, draft tube angle, guide vanes outlet angle, etc. After the selection of the geometric parameter for optimization, the next step is to define the limits on the design space to be studied. If, at the end of the first design iteration, the design goals are met on the edge of the design space for any variable, the design space should be adjusted further in that direction in an attempt to bring the maxima or minima into the design space (Schleicher and Oztekin, 2015). For determination of the iteration input values, a computational tool which includes basic optimization functions in order to rapid convergence to the optimal variable was used and new parameter was assigned manually to the solid model. For this study, part-by-part design and optimization strategy is adopted using CFD-based design methodology. In turbo machinery applications, it should be noticed that the maximum hydraulic efficiency is not reached at the design operation condition but at the best efficiency point (BEP). The target hydraulic efficiency is slightly lower than the maximum efficiency under the design head and design flow. The last step of the methodology is the structural verification for both manufacturing and operation processes. It should be indicated that the structural analysis is out of the scope of this work.

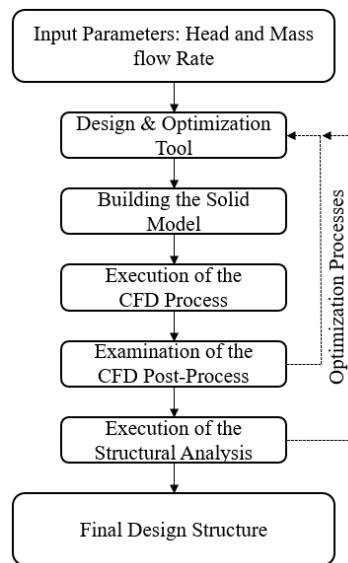


Figure 3. General design methodology of the turbo machinery components

Previous studies concerning energy generation in WSSs showed that one of the attractive solution is the implementation PATs (Giugni et al. 2013 ; Fontana et al. 2012). But both the water demand pressure and flow rate are not constant in WSSs. Turbines are generally designed for steady flow or low variations of flow and small changes can be adjusted by the guide vanes or similar components. Therefore, this high variation flow is not convenient to energy production using turbines, especially for Francis and Kaplan type turbines. Consequently, the present study will focus on PAT design for energy recovery in WSS.

For the design, three main characteristics should be known, design head, flow rate and rotational speed. After determination of these values, the specific speed of the pump can be calculated with the following equation:

$$n_s = 3,65 n \frac{Q_d^{1/2}}{H_d^{3/4}}, \quad (5)$$

where  $n$  is the rotational speed (rpm). The rotational speed of centrifugal pumps is between 50 and 200 rpm. Values of specific speed less than 50 are associated with radial type pumps. If the specific speed values are higher than 200, it represents semi-axial or axial blade profile (see Figure 4). An achievable hydraulic efficiency for the pump would be around 90%.

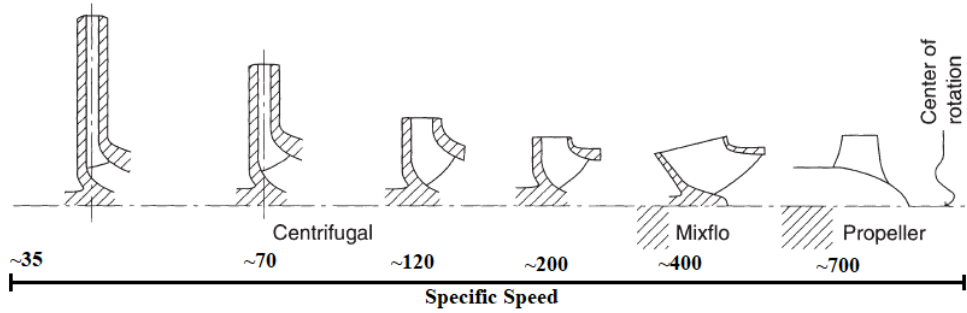


Figure 4. Effect of specific speed on the impeller geometry (Yedidiah, 1996)

For turbomachinery applications, the velocity triangles are used to represent the various components of velocities of the fluid at both the inlet and outlet sections. The flow around a blade is considered from the view of an observer sitting in the blade. Consequently, the relative velocities are relevant for the impeller, while the absolute velocities are used for the volute or diffuser calculation. The relationship between circumferential impeller speed  $U$ , relative velocity  $W$  and absolute velocity  $C$  is obtained from the rules of vector addition which can be illustrated as velocity triangles. The equations describing the geometry of triangles therefore apply to the calculation of all velocities, their components in circumferential or meridional direction and the angles  $\alpha$  and  $\beta$  (Gülich, 2008).

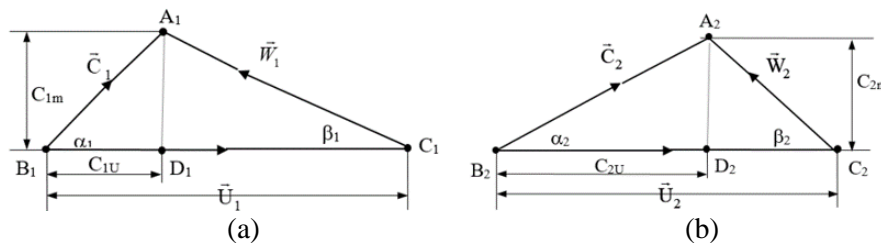


Figure 5. Velocity triangle drawn (a) for the inlet and (b) for the outlet

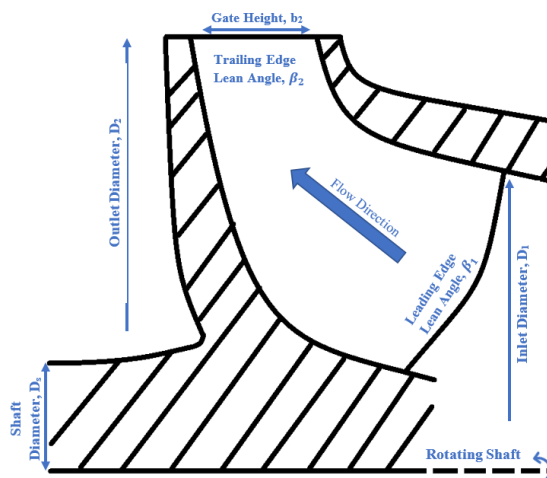


Figure 6. The basic dimensions of runner meridional channel

Many CFD based studies using  $k-\varepsilon$ ,  $k-\omega$  and  $SST k-\omega$  turbulence models are validated with the experimental model tests granting the validity of these models (Zeng et al, 2012; Choi et al, 2013, Anup et al, 2014; Teran et al, 2016).

The governing equations of the CFD analysis include the continuity equation (Ansys Inc, 2013);

$$\frac{\partial \rho}{\partial t} + \frac{\partial}{\partial x_j} (\rho U_j) = 0 \quad (6)$$

and the momentum equation;

$$\frac{\partial (\rho U_i)}{\partial t} + \frac{\partial}{\partial x_j} (\rho U_j U_i) = -\frac{\partial p'}{\partial x_i} + \frac{\partial}{\partial x_j} \left[ \mu_{eff} \left( \frac{\partial U_i}{\partial x_j} + \frac{\partial U_j}{\partial x_i} \right) \right] + S_m, \quad (7)$$

where  $S_M$  is the sum of body forces,  $p'$  is the modified pressure,  $\mu_{eff}$  is the effective viscosity so that:

$$\mu_{eff} = \mu + \mu_t, \quad (8)$$

where  $\mu_t$  is the turbulence viscosity.

The values of  $k$  and  $\varepsilon$  come directly from the differential transport equations for the turbulence kinetic energy and the turbulence dissipation rate:

$$\frac{\partial (\rho k)}{\partial t} + \frac{\partial}{\partial x_j} (\rho U_j k) = \frac{\partial}{\partial x_j} \left[ \left( \mu + \frac{\mu_t}{\sigma_k} \right) \frac{\partial k}{\partial x_j} \right] + P_k + \rho \varepsilon + P_{kb}, \quad (9)$$

$$\frac{\partial (\rho \varepsilon)}{\partial t} + \frac{\partial}{\partial x_j} (\rho U_j \varepsilon) = \frac{\partial}{\partial x_j} \left[ \left( \mu + \frac{\mu_t}{\sigma_\varepsilon} \right) \frac{\partial \varepsilon}{\partial x_j} \right] + \frac{\varepsilon}{k} (C_{\varepsilon 1} P_\varepsilon - C_{\varepsilon 2} \rho \varepsilon + C_{\varepsilon 3} P_{\varepsilon b}), \quad (10)$$

where  $C_{\varepsilon 1}$ ,  $C_{\varepsilon 2}$ ,  $\sigma_k$  and  $\sigma_\varepsilon$  are constants.

The idea of pump operating as turbine instead of turbines is a recent approach and researchers in turbomachinery field developed relations for obtaining pump characteristic curves of PATs. In general, presented relations were based on centrifugal pump's and turbine's best efficiency points and were verified by experimental data and theoretical analysis. Derakhshan and Nourbakhsh (2007) derived to predict BEP of PAT based on experimental studies. Characteristic curves of PATs can be obtained according to:

$$\frac{H_t}{H_{tb}} = 1.0283 \left( \frac{Q_t}{Q_{tb}} \right)^2 - 0.5468 \left( \frac{Q_t}{Q_{tb}} \right) + 0.5314 \quad \text{and} \quad (11)$$

$$\frac{P_t}{P_{tb}} = -0.3092 \left( \frac{Q_t}{Q_{tb}} \right)^3 + 2.1472 \left( \frac{Q_t}{Q_{tb}} \right)^2 - 0.8865 \left( \frac{Q_t}{Q_{tb}} \right) + 0.0452, \quad (12)$$

where subscripts  $p$ ,  $t$  and  $b$  refer to pump, PAT and BEP, respectively.

Coelho (2016) and European Small Hydropower Association (2014b) used empirical equations that calculate the efficiency in any flow characteristics for different kind of turbines. In the case of Francis turbines, peak or flow under-above efficiencies can be calculated with (European Small Hydropower Association, 2014b):

$$\eta_{F,\text{peak}} = \left[ 0.919 - \left( \frac{N_Q - 56}{256} \right)^2 + \left( 0.81 + \left( \frac{N_Q - 56}{256} \right)^2 \right) \left( 1 - \frac{0.789}{D_2^{0.2}} \right) \right] - 0.0305 + 0.005R_m, \quad (13)$$

$$\eta_{F,\text{below}} = \left[ 1 - \left( 1.25 \left( \frac{Q_{\text{peak}} - Q_t}{Q_{\text{peak}}} \right)^{3.94 - 0.0195N_Q} \right) \right] \eta_{F,\text{peak}}, \quad (14)$$

$$\eta_{F,\text{above}} = \eta_{F,\text{peak}} - \left[ \left( \frac{Q_t - Q_{\text{peak}}}{Q_d - Q_{\text{peak}}} \right)^2 (\eta_{F,\text{peak}} - (1 - 0.0072N_Q^{0.4})\eta_{F,\text{peak}}) \right], \quad (15)$$

where  $N_Q = k_2 H_d^{-0.5}$  is the different method for calculation of dimensionless specific speed,  $R_m$  is the turbine manufacture/design coefficient that can take values from 2.8 to 6.1. In case of Kaplan turbines, efficiency formulas are given by (European Small Hydropower Association, 2014b):

$$\eta_{K,\text{peak}} = 0.905 - \left( \frac{N_Q - 17}{700} \right) + \left( 0.095 + \left( \frac{N_Q - 170}{700} \right)^2 \right) \left( 1 - \frac{0.789}{D_2^{0.2}} \right) - 0.0305 + 0.005R_m, \quad (16)$$

$$\eta_K = 2 - \left[ 1 - \left( \frac{0.75Q_d - Q_t}{0.75Q_d} \right)^6 \right] \eta_{K,\text{peak}}, \quad (17)$$

where  $Q_{\text{peak}} = 0.75Q_d$ .

## 4. Numerical Studies and Case Study

### 4.1 The Napoli East Network

For the sake of validation, the previous described methodology was used to determine the most adequate and profitable site in the Napoli Est water distribution network for the installation of turbine or PATs, as previous presented in Fontana et al. (2012). Fontana and his co-workers investigate the use of pressure reduction valves and PATs for losses reduction and energy recovery in the Napoli Est network. The network is supplied by the San Sebastiano reservoir that presents a total storage volume of 30,000 m<sup>3</sup>. The distribution network is composed of 349 pipes with diameters ranging from 40 to 1000 mm and 251 nodes, from which 151 are demand nodes. Figure 7 schematically presents The Napoli Est WSS.

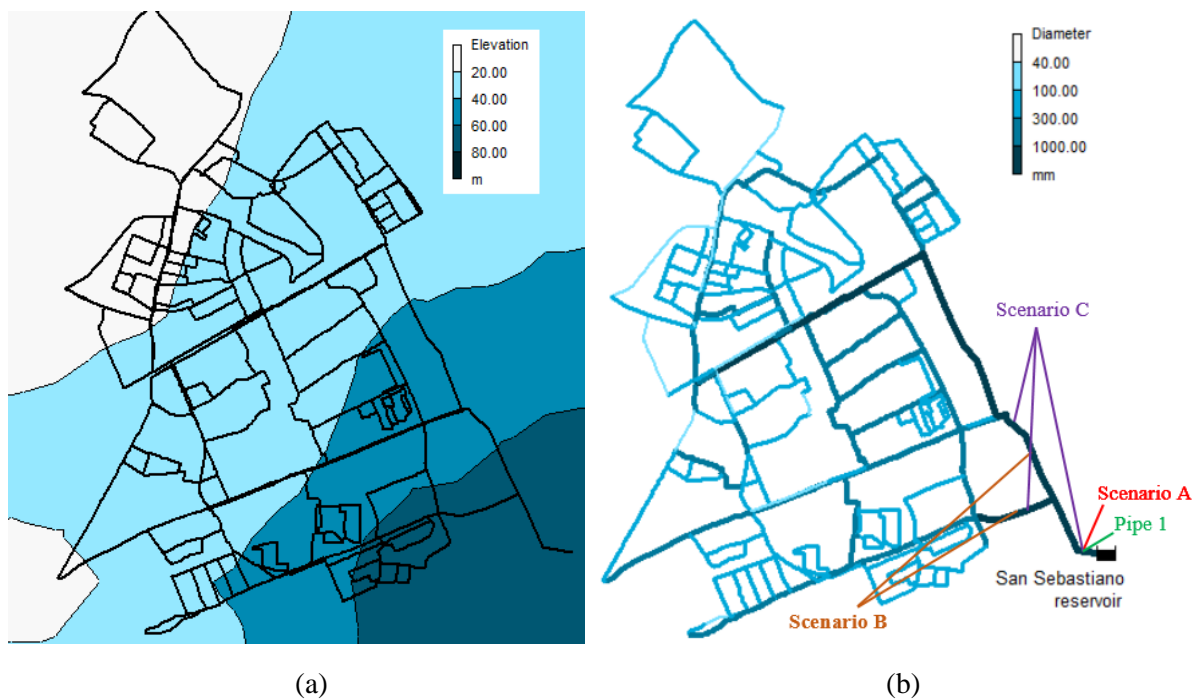


Figure 7. (a) Elevation map of the study area and (b) layout of Napoli Est water distribution system and locations of three scenarios. The Napoli Est water distribution system serves an area of approximately 920 hectares, covering most of the eastern zone of the city. The number of inhabitants is around 65,000-70,000 and the elevation ranges between 11-78 m above a sea level (Fontana et al., 2012)

Table 2. Results for the Napoli Est network (scenarios, A to C). Comparison with scenarios, S3, S6, S8 (Coelho and Andrade-Campos, 2017) and A<sub>F</sub>, B<sub>F</sub>, D<sub>F</sub> (Fontana et al, 2012).

Scenarios	Pipe ID	Head loss Coefficient Value	Dissipated Energy (kWh/day)	Flow Range, min-mean (l/s)	Head Loss, min-mean (m)	Total Dissipated Energy (kWh/day)
A	1	1450	964.8	229-337	6.54-14.19	964.80
B	P151	6100	507.6	115-169	6.67-14.5	999.84
	P198	6100	492.24	114-167	6.53-14.2	
C	1	1000	641.28	229-337	4.36-9.45	1001.76
	P151	2100	72.72	116-171	2.35-5.11	
	P198	2100	165.12	116-171	2.22-4.81	
S3	P354	3000	1694.25	219.6-299.4	11.94-22.73	1694.25
S6	P358	1000	16.9	53.70-73.69	0.48-0.92	16.9
S8	1	3000	1696.5	219.8-299.5	11.97-22.75	1696.5
A <sub>F</sub>	1	1000	723.47	232.8-324.2	0.30-0.41	723.47
B <sub>F</sub>	P151	94000	389.47	89.19-123.49	6.41-12.62	530.38
	P200	4000	140.91	29.91-41.37	6.95-13.63	
D <sub>F</sub>	P111	222000	2.26	3.18-4.01	1.43-2.30	817.76
	P134	114000	47.48	10.24-13.72	7.62-13.96	
	P354	1000	600.94	222.2-305.3	4.08-7.89	
	P358	73000	167.07	35.71-47.83	7.69-14.08	

After obtaining the hydraulic available power of each pipe of network using software EPANET 2.0 for all time steps of 1-day simulation, in order to create best scenarios for maximum energy recovery, flow-duration curves were drawn. An example is shown in Figure 8 for pipe 1. The flow-duration curve of pipe 1 showed that the mean flow is  $\sim 0.36 \text{ m}^3/\text{s}$  and minimum flow for an entire day is  $0.23 \text{ m}^3/\text{s}$ . These results are important to understand the flow regime of the pipes. In general, turbines are designed by taking into consideration constant flow rate and rotational speed values. However, in WSSs, flow characteristics are not stable and this situation requires deep technical feasibility studies. Three different scenarios were created, which include varying number and locations for PRVs (see Figure 7b). The solutions for the optimization problem expressed in Equations 3 and 4 are listed in Table 2, where minor head loss values for PRVs were assigned. The minimum head pressure of nodes was determined as 20 m for present study. These scenarios are compared with the previous studies of Fontana et al. (2012)



and Coelho (2016). However, the main objective of Fontana et al. (2011) was to find optimal locations for installing PRVs in order to minimize the water losses in the network while maintaining the required minimum pressure at the demand nodes. Authors defined 25 m as the minimum head pressure for the demand nodes. Then, the objective was to find a possible replacement of such valves by PATs in order to recover the energy that is dissipated by the valves. In the study of Coelho (2016), the aim was to develop a tool for the determination of potential sites. The developed tool also included technical/financial analyses and it was used for the selection of adequate hydraulic turbine for the maximum energy production. PATs were not considered. Fontana et al (2012) aimed to reduce water leakages, do not maximize energy production.

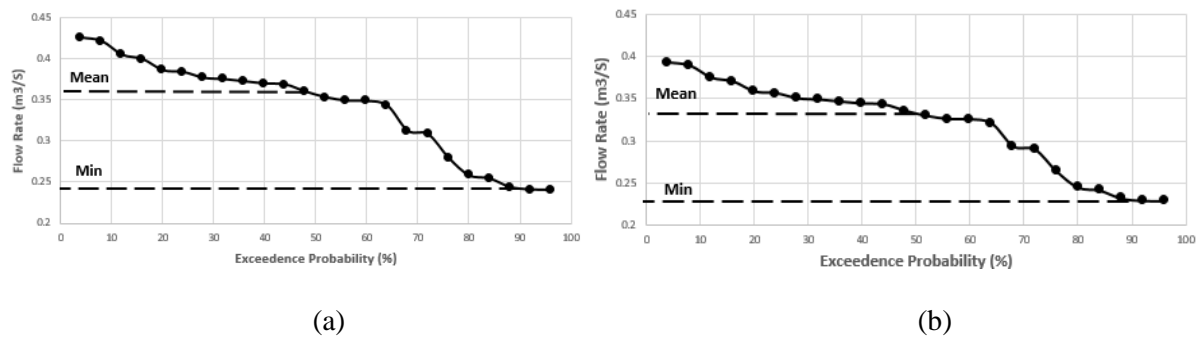


Figure 8. The flow duration curves of pipe 1 (a) before and (b) after the PRV implementation

Six different scenarios were created and the PRV implementation results showed that the recoverable energy of pipe 1 is 723.35 kWh/day when head loss coefficient is defined as 1000. Coelho (2016) only took into consideration minimum pressure values on nodes with non-zero water demand. This situation allows to obtain head loss coefficients for pipe 1 as 3000 and the dissipated energy of PRV of 1696.5 kWh/day. However, minimum pressure for the whole network is defined as 20 m for present study and the results of PRV implementation into pipe 1 showed that the maximum dissipated energy can only be 968.8 kWh/day.

The main objective of Fontana et al. (2012) was the reducing of leakages of network. Therefore, dissipated energies from all scenarios are less than other created scenarios. The authors also indicated that when increasing the number of PRVs, the potentially recovered energy can even decrease depending on the pipe on which the PATs would be installed.

## 4.2 Technical Feasibility Results

The main purpose of this study is the recovery of the maximum energy and this should be analyzed via technical analysis. Technical analysis allows us to evaluate which type of turbine is the best for maximize energy recovery. The first step in the selection of turbines for a specific site consists in the selection of the types of turbines that operate in the range of available head (Coelho, 2016). The selected type of turbines, efficiencies and total recoverable energies for each scenario are given in Table 3. In preliminary technical analysis, PATs hydraulic efficiency is assumed as 70%.

As it can be seen from Table 3, Scenario A and Scenario B are divided into three different design options 1, 2 and 3 and their recoverable energies using PATs, Francis or Kaplan type turbines respectively. For Scenario C, PATs and Kaplan turbines combinations are selected and tested. Scenario A is chosen particularly for the analysis of pipe 1, which has the highest flow rate among all network. More than one turbine selection and parallel installation projects are possible in cases such as this one.

Contrary to expectations, the highest total dissipated energy is obtained by Scenario C, which has three different sites: pipes 1, P151 and P198. Pipes P151 and P198 are placed after the main pipe of reservoir and the results of flow-duration curves of these pipes showed that the flow regimes are similar, meaning that these pipes separate equally the flow that comes from reservoir. In this case, similar turbines or PATs can be installed.

In all scenarios, the Kaplan/Propeller-type turbines demonstrated to be the most efficient. However, when selecting a turbine, the range of flows operation should also be taken into account since distinct turbine types present distinct efficiency variations when operating at flow rates outside the design flow. The Kaplan turbine incorporates one essential feature not found in other turbine rotors: the setting of the stagger angle. At part load operation, the setting angle of the runner vanes is adjusted automatically by a servomechanism to maintain optimum efficiency conditions (Dixon and Hall, 2014).

Table 3. Technical pre-analysis results of daily net energy production for each scenario. The results of Coelho and Andrade-Campos (2017) are also presented for comparison purposes

Scenarios	Pipe ID	Dissipated Energy (kWh/day)	Type of Turbine	Turbine Efficiency	Total Recv. Energy (kWh/day)
A1	1	964.8	Francis	0.731	705.27
A2	1	964.8	PATs	0.700	675.36
A3	1	964.8	Kaplan	0.887	855.78
B1	P151	507.6	Francis	0.678	677.89
	P198	492.24	Francis	0.678	
B2	P151	507.6	PATs	0.700	699.89
	P198	492.24	PATs	0.700	
B3	P151	507.6	Kaplan	0.883	882.86
	P198	492.24	Kaplan	0.883	
C	1	641.28	Kaplan	0.872	725.75
	P151	72.72	PATs	0.700	
	P198	165.12	PATs	0.700	
S3	P354	1694.25	Francis	0.790	1338.57
			Kaplan	0.894	1514.48
			Cross-Flow	0.790	1338.48
S8	1	1696.5	Francis	0.790	1340.54
			Kaplan	0.894	1516.47
			Cross-Flow	0.790	1340.24

### 4.3 Pump Design and CFD Validation

In this study, the design parameters were determined as  $Q_d=0.1 \text{ m}^3/\text{s}$ ,  $H_d=12.2 \text{ m}$  and  $n=1450 \text{ rpm}$ . Using these parameters in Equation 1, the available hydraulic power can be calculated of 10.77 kW input power. The selected design parameters are then used to dimension some basic geometric parameters for a preliminary design such as runner inlet diameter ( $D_1$ ), outlet diameter ( $D_2$ ), shaft diameter ( $d_s$ ).

By using the design parameters of Equation 5, the dimensionless rotational speed is calculated as 256.4 rpm. At the trailing edge of the blade, the diameters are assumed to be the same at the hub and shroud.

The number of blades calculated is 7 and thickness of blades is 5 mm. The calculated radiuses and angles of both the trailing and leading edges are given Figure 9a.

Numerical simulations were performed to calculate hydraulic efficiency of full turbine. For this purpose, the design methodology presented in Figure 9a was adopted. The blade geometry was created by using ANSYS Bladegen V16.1, which allows to create the meridional profile of a blade and a solid model can be parameterized for detailed design simulation. The meridional profile created for this study is shown in Figure 9b. The computations were carried out with ANSYS CFX using the steady-state solver method with multiple frames of reference for single blade analysis.

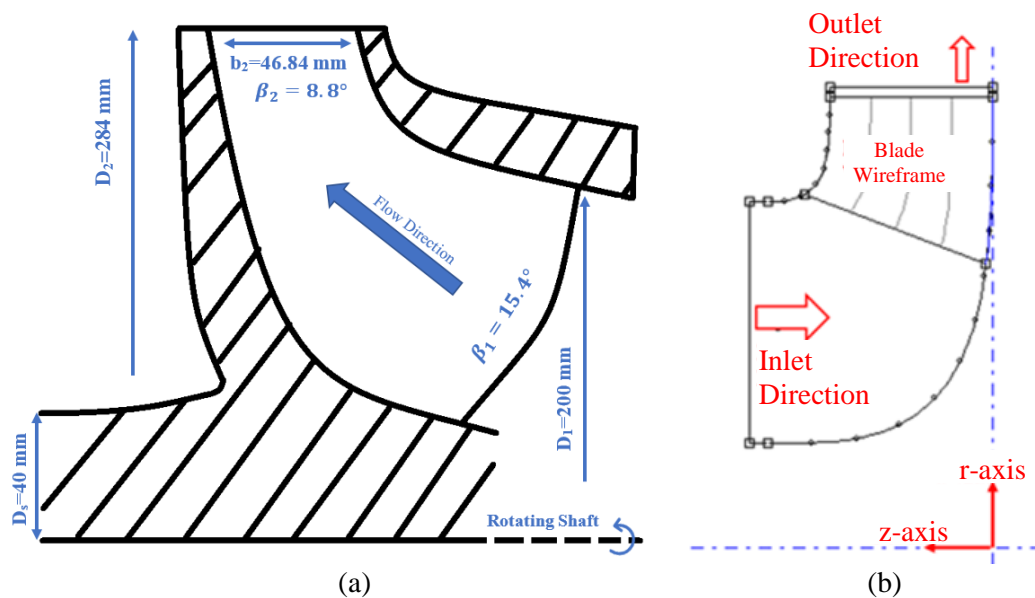


Figure 9. (a) Dimensions of preliminary pump runner meridional channel and (b) meridional profile by ANSYS Bladegen 16.1

After building the CAD model of the runner, the element discretization model has been created using by ANSYS Meshing using fine mesh quality and tetrahedron type mesh. The complete domain was represented by 671284 elements, where 531525 of total elements compose the runner. In the CFX setup,  $k-\varepsilon$  turbulence model has been selected.

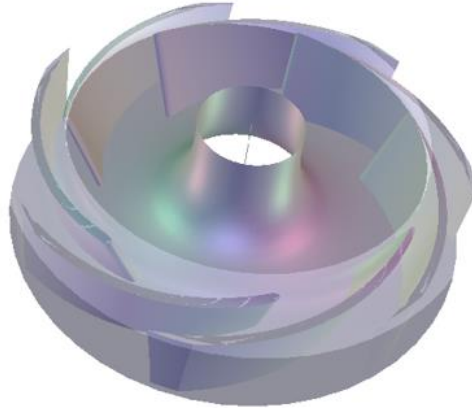


Figure 10. 3-D Illustration of the preliminary runner design

The boundary conditions of a full turbine are listed in Table 4. The outlet was set as mass flow rate, the inlet flow condition was set as total pressure and velocities were chosen normal to the boundary surface. Pipes, hub and shroud curves and blade surfaces were assumed as non-slip wall boundary conditions.

In CFD applications different types of validations are required to ensure the accuracy of analysis. For this reason, in this study, RMS residuals, flow rate check, net head re-calculation using computed inlet pressure and minimum absolute pressure controls were used. A mesh grid independence test also made for single blade and full turbine geometry. A RMS residual criterion was set to  $10^{-5}$ , being achieved in all simulations.

Table 4. Boundary conditions of the full geometry

Boundary Area	Boundary Condition
Inlet	Total Pressure
Outlet	Mass Flow Rate
Hub-Shroud	No Slip Wall
Impeller Blades	No Slip Wall
Pipe 1 – Pipe 2	No Slip Wall

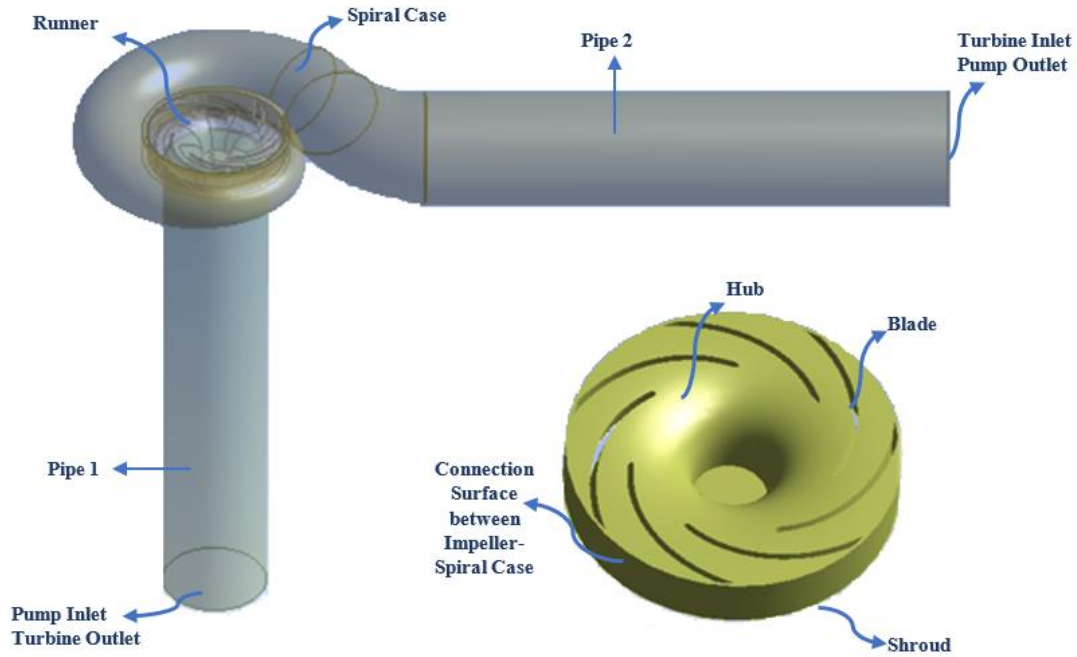


Figure 11. Full turbine geometry

The hydraulic efficiency of the runner was found to be 90% for the preliminary design. However, single blade analyses showed that the hydraulic efficiency of the blade is 84.1%. A response surface optimization methodology was applied on blade geometry.  $B_2$  gate height and  $D_2$  outlet diameter, leading and trailing edge lean angles were manipulated and a single blade efficiency was increased to 89.6%.

Table 5. Optimization design parameters

Geometric Parameter	Preliminary Design	Final Design
Gate Height, $b_2$ (mm)	42.93	46.84
Outlet Diameter, $D_2$ (mm)	284	260
Leading Edge Lean Angle, $\beta_1$ ( $^\circ$ )	15.4	19
Trailing Edge Lean Angle, $\beta_2$ ( $^\circ$ )	8.8	19

The relative velocity streamlines were almost parallel to the circumferential velocity component in the preliminary design case. This situation indicates a problem on the leading edge angle and the shroud zone. In the optimization process, relative velocity streamlines (monitored as a velocity in stationary

frame on Figure 12) around shroud zone were controlled and velocity streamlines took a form as the velocity triangles.

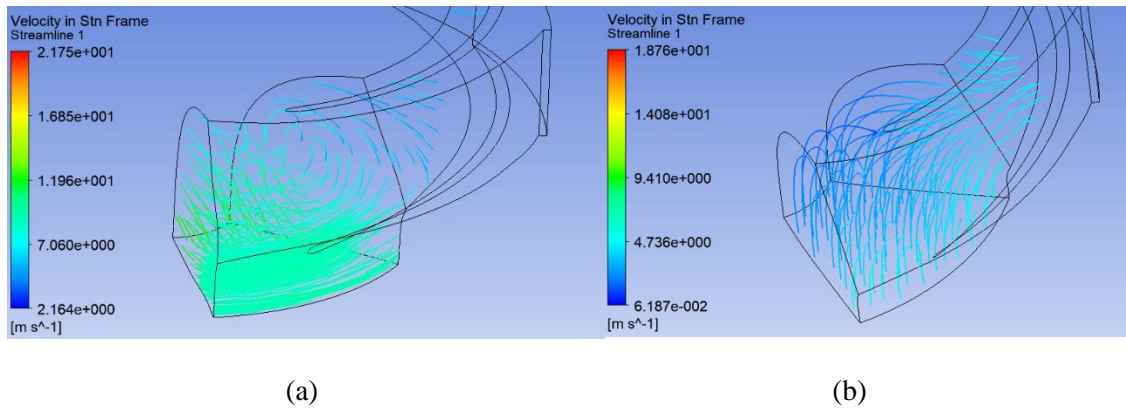


Figure 12 Single Blade Analysis Relative Velocity Streamlines (a)Preliminary Design (b)Final Design

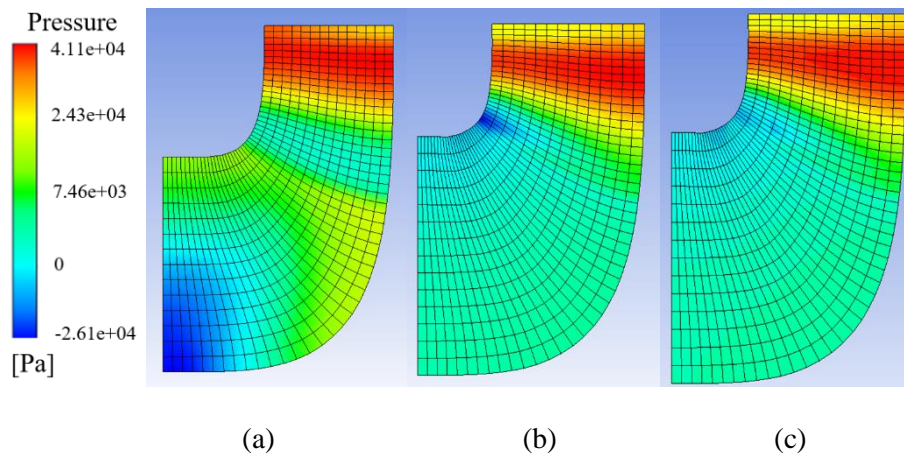


Figure 13 Single Blade Analysis Meridional Profile Pressure Distributions (a) Preliminary Design (b) Improved Design (c) Final Design

Figure 13 shows a comparison of the pressure contours on the meridional profile for the observation of pressure distribution. It is clearly seen that the unbalanced pressure distributions of the fluid have been eliminated, which indicates reduced energy losses and increased turbine efficiency.

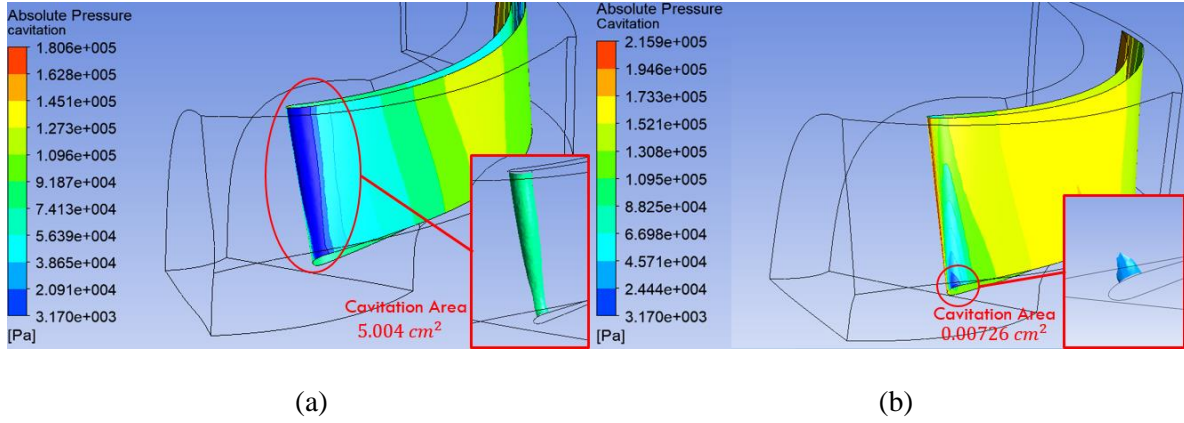


Figure 14 Single Blade Analysis Absolute Pressure Distributions and Cavitation Control (a) Preliminary Design (b) Final Design

The geometric parameters used in the optimization process are listed in Table 5. Optimization studies also include cavitation control. In the preliminary designed blade geometry, very big cavitation regions are observed on the trailing edge. However, with small modifications on the design of impeller and by considering CFD simulation results, the cavitation regions were decreased in the acceptable limits (Figure 14).

The final design was analyzed and the best efficiency point (BEP) was determined as  $Q_{BEP}=84$  l/s,  $H_{BEP}=13.43$  m and the efficiency of pump  $\eta_{BEP}$  is 81.2% at 1450 rpm. Pump power  $W_{BEP}$ , at BEP was calculated as:

$$W_{BEP} = \rho g H_{BEP} Q_{BEP} \eta_{BEP} \cdot \quad (18)$$

The CFD results at 1450 rpm are given in Figures 15 and 16. The power is the product of the torque and the angular velocity of generator shaft. On the other hand, hydraulic efficiency is the function of head, torque and mass flow rates. The pump characteristics curve of CFD reveals that there is an increase in efficiency with respect to decrease of head, similarly the same reflects for torque and power.

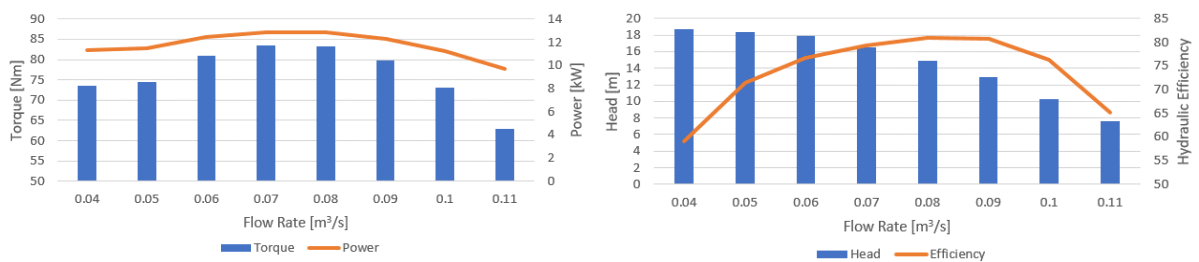


Figure 15. Full pump analysis results at 1450 rpm



Pressure distributions at the axial plane and meridional plane for BEP operation condition are shown on Figure 16. Pressure differences from the pressure and suction sides are higher at the higher load and these differences result in torque on the shaft. On meridional profile, gradually pressure can be seen and static pressure difference between leading and trailing edge is around 114 kPa (equal to 11.4 m head). The total pressure difference between system inlet and outlet is around 143 kPa but it should not be forgotten that pressure fluctuations are usually a result of a vortex created in spiral case at the outlet of around runner. This situation causes pressure losses in the spiral case and total pressure decreases until reaching system outlet. Nevertheless, pressure drops can be reduced with geometric optimizations as much as possible. For this study, total pressure drop between spiral case inlet and system outlet is approximately 13 kPa, being this value acceptable for non-slip wall function analysis.

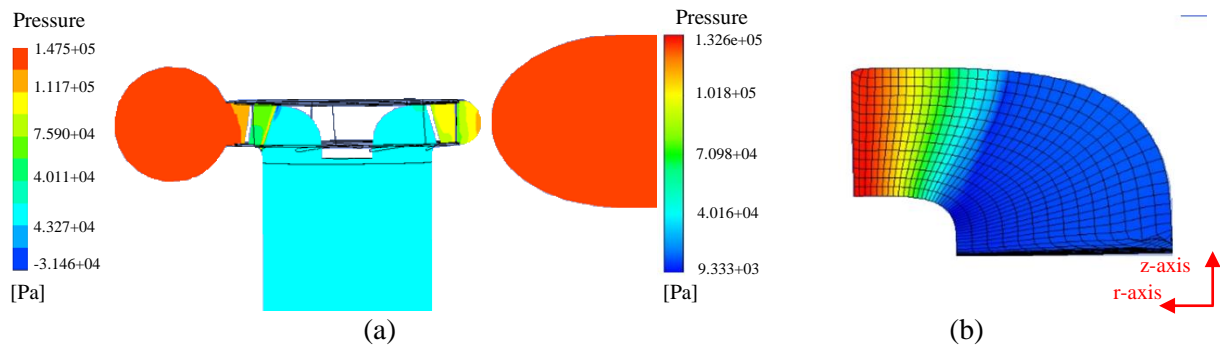


Figure 16. Results of the final design (a) total pressure contours of the full pump and (b) pressure contour of the meridional plane of the runner

#### 4.4 PAT CFD Analysis

In the case of PATs CFD analysis, boundary conditions are reversed with a centrifugal pump running in reverse. When operating in reverse, outlet boundary of the pump is defined as a total pressure inlet. PAT characteristic curves that show the relationship between head-flow rate and power-flow rate were obtained by Equations 11 and 12. Scenario B2 was chosen for PAT installation due to the flow profile. Flow characteristics of pipe P198 are in a good agreement with operation range of the designed pump. Pipe P151 has also a flow profile similar of pipe P198 as it can be seen by the FDC curves in Figure 17. Thus, PATs which have the same design can be installed on both pipes P151 and P198.

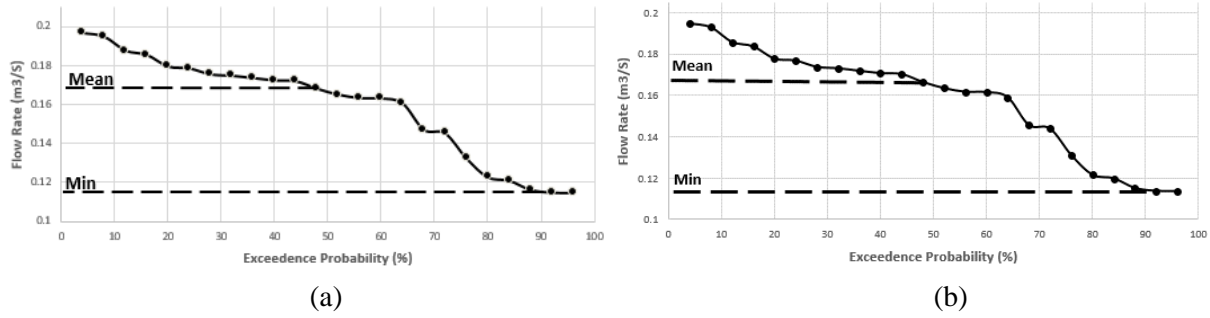


Figure 17. Flow duration curves of pipes (a) P151 and (b) P198 after the PRV implementation

Numerical simulations were performed to analyze PATs operation with pipe P198 and to obtain produced power of each time step. The results of the simulations for the Scenario B2 are given in Table 6.

Flow characteristics of the network for 1-day simulation showed that in night operation, between 2 and 6, the flow rates of pipes are under the minimum operation range ( $0.06 \text{ m}^3/\text{s}$ ) when considering two PAT. Therefore, the produced energy would be set to zero if two PATs would operate at the same time. However, the values which were located on station before and after the turbines allow to turn one pump off while operating another turbine. CFD analysis boundary conditions are determined for a single PAT operation in day time between 2 and 6 am. By this way, the produced power by a single PAT was obtained higher than other parallel turbine operation hours, because of their higher flow rate values. It was expected that for operations higher than  $0.13 \text{ m}^3/\text{s}$  the same idea would be applied. However, this is not possible while rotating the generator at a constant rotational speed. For this study, rotational speed is defined as 1450 rpm. The selection of lower or higher rotational speed values can affect positively to both the hydraulic efficiency and the produced power in some timesteps. However, the operation limits of the PAT also increase or decrease with respect to variation of the rotational speed. The hydraulic efficiencies in the rest of timesteps may also be reduced by this manipulation.

For reaction turbines, it should not be forgotten that pressure drop increases with the flow rate. Nevertheless, head pressure on the nodes in the network never decreases below 14.2 m in the given circumstances, being acceptable for the timesteps between 2 and 6 am.

CFD results showed that the total produced energy with a PAT in pipe P198 is 418.6 kWh/day. The total produced energy for Scenario B2 can be assumed as 837.2 kWh/day because of the similarity of

Flow Duration Curves, which are given in Figure 17. The overall PATs efficiency was calculated and the values of 66% was obtained. These values are lower than the value of the BEP. Technical results showed that the recoverable daily energy was 699.89 kWh/day when PATs efficiency is assumed as 70% (Table 3). Nevertheless, daily production at the end of the CFD analysis is higher because of the single pump operation and the weighted efficiency become slightly close to BEP.

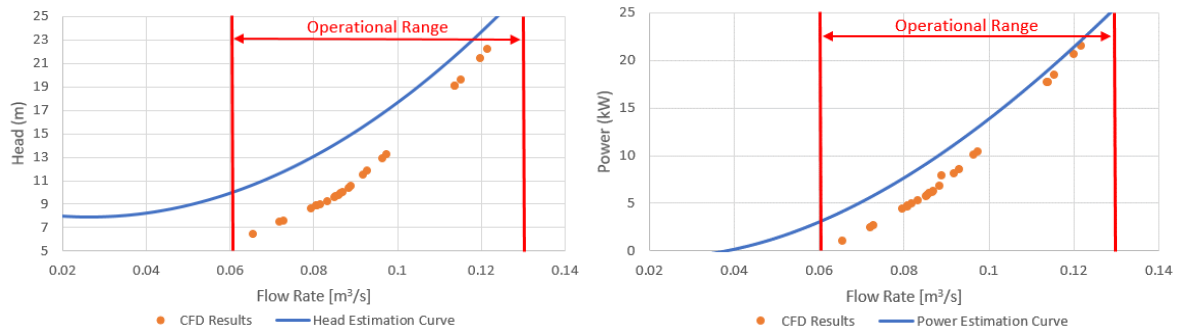


Figure 18. Comparison of the CFD result with the estimation curve (see Equation 11 and 12)

In figure 18, the produced power and head drop that were numerically obtained were compared with the curves computed from Equation 12. As it can be seen from the figure, the numerical results are slightly under the estimation curve. This difference can be caused by two reasons. First, Derakhshan and Nourbakhsh (2007) developed this relations for the centrifugal pumps. However, the designed pump in this study has a semi-axial blade profile. The second reason is related to possible numerical errors, mainly coming from the finite precision of computations and the truncation errors.

Kaplan turbine efficiency curve (Scenario B3) and PAT efficiency curve (Scenario B2) are given in Figure 19. As it can be seen in Figure 19a, Kaplan turbine provides almost stable hydraulic efficiency. At same operating conditions, the designed PAT have larger oscillations during operation period (Figure 19b).

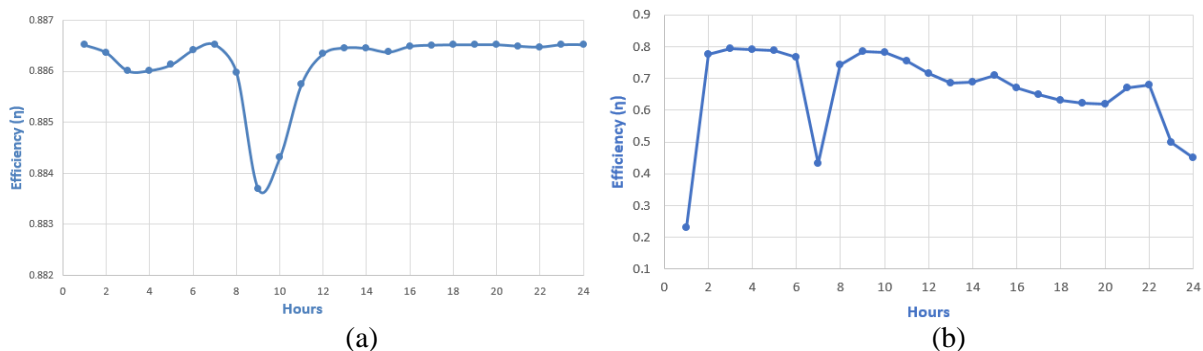


Figure 19. Turbine installation efficiency curves for (a) Scenario B3, where Kaplan Turbines were applied (Obtained by Equation 16 and 17), and for (b) Scenario B2, where particular designed PATs where applied

Table 6. Numerical results of the PAT and comparison with the estimated head and power values that are obtained from Equation 11 and 12.

Time Step	Flow Rate in Pipe (m <sup>3</sup> /s)	Number of PAT Operating	Estimated Head for Each PAT (m)	Estimated Power for Each PAT (kW)	Rotational Speed (rpm)	PATs Hydraulic Efficiency	Head loss in Pipe	Produced Energy by PAT (kWh)	Produced Energy in Pipe 198 (kWh)
1	0.1311	2	10.67	4.21	1450	23%	6.42	1.10	2.19
2	0.1199	1	23.65	21.37	1450	77%	21.44	20.72	20.72
3	0.1137	1	21.64	18.91	1450	79%	19.06	17.70	17.70
4	0.1138	1	21.66	18.95	1450	79%	19.1	17.75	17.75
5	0.1152	1	22.12	19.51	1450	79%	19.6	18.52	18.52
6	0.1216	1	24.23	22.06	1450	77%	22.17	21.58	21.58
7	0.1439	2	11.65	5.65	1450	43%	7.47	2.51	5.01
8	0.1836	2	15.62	11.19	1450	74%	11.51	8.19	16.37
9	0.1947	2	16.98	13.00	1450	78%	13.21	10.49	20.98
10	0.1929	2	16.75	12.69	1450	78%	12.91	10.10	20.20
11	0.1858	2	15.87	11.53	1450	76%	11.82	8.63	17.26
12	0.1777	2	14.94	10.27	1450	72%	10.5	7.96	15.92
13	0.1731	2	14.42	9.57	1450	68%	9.89	6.24	12.47
14	0.1737	2	14.50	9.67	1450	69%	9.97	6.35	12.71
15	0.1768	2	14.83	10.13	1450	71%	10.38	6.90	13.80
16	0.1707	2	14.17	9.23	1450	67%	9.67	5.86	11.73
17	0.1664	2	13.73	8.61	1450	65%	9.24	5.32	10.64
18	0.1635	2	13.42	8.19	1450	63%	8.99	4.95	9.90
19	0.1617	2	13.25	7.95	1450	62%	8.85	4.74	9.49
20	0.1615	2	13.24	7.92	1450	62%	8.84	4.72	9.44
21	0.1702	2	14.12	9.16	1450	67%	9.58	5.80	11.60
22	0.1719	2	14.29	9.39	1450	68%	9.75	6.04	12.09
23	0.1591	2	13.00	7.59	1450	50%	8.64	4.41	8.82
24	0.1456	2	11.79	5.86	1450	45%	7.6	2.71	5.43

## 5. Financial Analysis

The financial costs of Francis and Kaplan turbines were obtained from the equations shared by Natural Resources Canada (2005). Despite the fact that the designed pump has not the same characteristics with Caprari NC 150-200, the investment costs of PATs are considered similar as the Caprari NC 150-200 provided by Fontana et al. (2012) for comparison. According to the Colorado Energy Office (2015), the operation and maintenance costs were assumed as 10 % of the project's total annual income. The energy tariff considered to compute the annual income was the Italian tariff, defined as 0.220 €/kWh (Fontana et al. 2012).

Table 7. Annual income and investment costs

Scenarios	Type of Turbine	Total Recovered Energy (MWh/year)	Annual Income from Energy Production (€)	Investment Costs (€)
A1	Francis	257.59	56,671	138,306
A2	3 PATs	246.67	54,267	117,000
A3	Kaplan	313.62	68,997	149,666
B1	Francis	247.59	54,471	79,699
	Francis			79,699
B2	2 PATs	305.78	67,272	78,000
	2 PATs			78,000
B3	Kaplan	325.01	71,503	90,767
	Kaplan			90,767
C	Kaplan	266.22	58,569	139,700
	2 PATs			78,000
	2 PATs			78,000

As shown in Table 7, Scenarios A and B were divided into different scenarios that can be chosen in order to install optional turbine types. Kaplan turbines offer the highest recovered energy of both scenarios; however, the engineering and manufacturing costs are higher than the other turbines type as well. Francis turbines, that operate efficiently in high head values, might be a good choice because this type of turbines can response to sudden flow characteristic changes such as the observed in WSSs

through guide vane components. However, the technical results show that the operation of the Francis turbines with low-head operation result in low energy production and consequently, small incomes.

Total investment costs of PATs are slightly close to the turbine costs. However, the time required for design and manufacturing processes should be taken into account for the case of Kaplan and Francis turbines. Therefore, this process would be time-consuming and investors could choose PATs to shorten this process, rather than alternative projects that would not obtain large profit in the future.

Table 8. Preliminary income analysis

Scenarios	Annual Operation and Maintenance Cost (€)	Annual Net Profit (€)	Breakeven Point (Years)	Income After 15 Years (€)
A1	5,667	51,004	2.71	626,748
A2	5,427	48,841	2.40	615,610
A3	6,900	62,097	2.41	781,795
B1	5,447	49,024	3.25	657,665
B2	6,727	60,545	2.58	853,077
B3	7,150	64,353	2.82	891,012
C	5,857	52,712	5.61	582,831

Comparing Scenario B3 with the others, although it presents the highest annual O&M costs, the Kaplan turbines present the highest income after 15 years. Contrary to the expectations, the PATs designed in this study (Scenario B2) presents one of the highest annual income in comparison to other scenarios. Investors who want to make long-term or short-term investments may prefer this scenario because the breakeven point is slightly close to the smallest breakeven point. Scenario B2 also offers the second highest income in Table 8.

## 6. Conclusions, Contributions and Recommendations

In this work, in order to compute the flow characteristics of any water supply systems, a numerical methodology was proposed. A numerical tool that analyzes a hydraulic model and modify it for the required analysis was developed. These approaches consider the collection of pressure and flow data in calculations and identify suitable locations for the maximization of the energy recovered using hydro turbines.

This study also includes design of selected type turbine and its performance analysis. Computational fluid dynamics method is used for the determination of hydraulic performance of turbine. The input design parameters which involve flow rate and head are determined for a preliminary design and CFD-based optimization studies are started for the maximization efficiency. Then, the designed turbine is analyzed to determine the daily available power of the scenario. These results are used in pre-financial analysis in order to compare the scenarios.

The Napoli Est region in eastern Italy is selected as case study. The developed tool searched for available locations for the installation of distinct types of turbines with the aim of maximize the energy recovery. Three sites are selected in this region according to their different flow characteristics, different type turbines and different operation strategies (parallel or single turbine operations). One of these scenarios was selected for PATs installation and a new pump was designed, taking into consideration the pump characteristics of preliminary studies. CFD-based optimization studies are also applied for the pump operation. Next, the PAT is analyzed to determine the available power of the reverse operation condition during one-day simulation of network. Financial analysis has revealed the scenario to get the best income in short-term or long-term period.

The main conclusions of this work are as follows:

- Water supply systems allow to obtain widespread and significant amount of energy recovery.
- Reservoirs are usually located at a highest point of sites so the water can pass by gravity through the network. A large drop in elevation between the reservoir and the network may produce a large pressure in pipes.

- Hydro turbines are designed to operate for small variations of flow characteristics. However, Kaplan turbines can be easily adapted due to the setting of the stagger angle.
- Pump as Turbines are the effective solution for producing energy in water supply systems. The efficiency of PATs is usually lower than that of conventional turbines however, they also have multiple advantages as a low cost, easy installation and time saving.
- The application of parallel installation of turbines allows to turn one turbine off and high energy production values can be achieved with this operation. It should not be forgotten that, as the flow rate used by the reaction turbines increases, the pressure drops also increases parabolically and the minimum pressure in entire network might be under comfort ranges.
- Case study showed that PATs are an attractive opportunity for long-term investment.

The main advantages, achievements and contributions of this study are listed as follows:

- The implementation of micro hydro turbines in the water supply system via detailed investigation at selected sites shows that the energy production could be possible using renewable energy solutions.
- The developed tool has the advantage of considering turbine type such as Kaplan, Francis or PAT turbine as well as site characteristics such as the best energy recover locations which is not the case in the classical pressure management methods.
- This study investigates a usage of Pump as Turbine in a variable operating condition using computational fluid dynamics methods in water supply systems.
- The proposed approach analyzes different scenarios (different site location and different type turbine selection) along with a financial analysis. Such a detailed analysis determines whether the balance of costs and savings of a certain scenario is attractive.

The following works are recommended for future studies:

- In this study, the tool is developed for the determination of suitable sites for energy production. In order to find these locations, the PRV implementation methodologies are used because of EPANET limitations. Using a more advanced program, faster and more precise results can be



obtained for the investigation of the turbine installation with an inclusion of turbine efficiency curves instead of PRV implementation process.

- In this study, optimization techniques were applied to PAT into consideration only pump operation. In literature, different studies have been published concerning energy production using PATs, which have been combined with some design optimizations to maximize energy. Recovered energy can be increased using these optimization techniques and PATs can be the first option to produce energy from WSSs with low investment costs.

## 7. References

- Acharya N., Kim C., Thapa B., Lee Y., Numerical analysis and performance enhancement of a cross-flow hydro turbine, *Renewable Energy* 2015, 80, 813-826.
- Ansys Inc. CFX solver theory guide. Release 2013, 15, 79-90.
- Anup KC, Thapa B, Lee Y. Transient numerical analysis of rotor-stator interaction in a Francis turbine. *Renewable Energy* 2014, 65, 227-235.
- Bovet T. Contribution to the study of Francis – Turbine Runner Design. Lausanne; 1963.
- Carravetta A., Giudice G.D., Fecarotta O., Ramos H.M., Energy production in water distribution networks: A PAT design strategy, *Water Resour Manage*, 2012, 26, 3947–3959.
- Choi H, Zullah MA, Roh H, Ha P, Oh S. CFD validation of performance improvement of a 500 kW Francis turbine, *Renewable Energy* 2013, 54, 111-123.
- Coelho B., Energy efficiency of water supply systems using optimization techniques and micro-hydropower, PHD Thesis, Universidade de Aveiro, 2016.
- Coelho B., Andrade-Campos A., Efficiency achievement in water supply systems—A review, *Renewable and Sustainable Energy Reviews*, 2014, 30, 59–84.
- Coelho B., Andrade-Campos A., energy recovery in water networks: numerical decision support tool for optimal site and selection of micro turbines, in press, 2017.
- Corcoran L., McNabola A., Coughlan P., Optimization of water distribution networks for combined hydropower energy recovery and leakage reduction, *Journal of Water Resources Planning and Management*, 2016, 142, 2.

Derakhshan S., Nourbakhsh A., Experimental study of characteristic curves of centrifugal pumps working as turbines in different specific speeds, *Experimental Thermal and Fluid Science*, 2008, 32, 800-807.

Deyou L., Hongjie Q., Gaoming X., Ruzhi G., Xianzhu W., Zhansheng L., Unsteady simulation and analysis for hump characteristics of a pump turbine model, *Renewable Energy* 2015, 77, 32-42.

Dixon S.L. Hall C.A., *Fluid Mechanics and Thermodynamics of Turbomachinery (Seventh Edition)*, Elsevier Inc, 2014.

EPANET, United States Environmental Protection Agency, [Online, 2017], Available from : <https://www.epa.gov/water-research/epanet>

European Small Hydropower Association. (2004b). Guide on how to develop a small hydropower plant (Part 2). Retrieved 2015, Available from : [https://energypedia.info/images/4/4a/Part\\_2\\_guide-on\\_how\\_to\\_develop\\_a\\_small\\_hydropower\\_plant-final-21.pdf](https://energypedia.info/images/4/4a/Part_2_guide-on_how_to_develop_a_small_hydropower_plant-final-21.pdf)

Fecarotta O., Carravetta A., Ramos H.M., CFD and comparisons for a pump as turbine: Mesh reliability and performance concerns, *International Journal of Energy and Environment*, 2011, 2, Issue 1, 39-48.

Fontana N., Giugni M., Portolano D., Losses Reduction and energy production in water distribution networks, *Journal of Water Resources Planning and Management*, 2012, 138, 3.

Giugni M., Fontana N., Ranucci A., Optimal location of PRVs and turbines in water distribution systems, *Journal of Water Resources Planning and Management*, 2013, 140, 9.

Gulich J.F., *Centrifugal Pumps*, Springer Berlin Heidelberg New York, 2008.

McBride M.W., *The design and analysis of turbomachinery in an incompressible, steady flow using the streamline curvature method*, Technical Memorandum, 1979.

Miloş T., Bărglăzan M., CAD technique used to optimize the Francis runner design, *The 6th International Conference on Hydraulic Machinery and Hydrodynamics* 2004.

Natural Resources Canada. (2005). Clean Energy Project Analysis: RETScreen Engineering & Cases Textbook (3rd ed.). Retrieved 2015, from [http://publications.gc.ca/collections/collection\\_2007/nrcan-rncan/M154-13-2005E.pdf](http://publications.gc.ca/collections/collection_2007/nrcan-rncan/M154-13-2005E.pdf)

Patelis M., Kanakoudis V., Gonelas K., Pressure management and energy recovery capabilities using PATs., *Procedia Engineering* 2016, 162, 503-510.

Patermann H., *Strömungsmaschinen*, Springer-Verlag, Berlin, 1964.

Perez-Sanchez M., Sanchez-Romero F., Ramos H.M., Lopez-Jimenez P.A, Energy Recovery in Existing Water Networks: Toward Greater Sustainability, *Water* ,2017, 9, 97.

Ramos H.M., Mello M., De P.K., Clean power in water supply systems as a sustainable solution: from planning to practical implementation, *Water Science and Technology, Water Supply*, 2010, 1, 39-49.

Ramos H.M., Kenov K.N., Vieira F., Environmentally friendly hybrid solutions to improve the energy and hydraulic efficiency in water supply systems, *Energy for Sustainable Development*, 2011, 15, 436-442

Schleicher W.C., Oztekin A. Hydraulic design and optimization of a modular pump-turbine runner, *Energy Conversion and Management* 2015, 93, 388–398

Teran L.A., Larrahondo F.J., Rodriguez S.A., Performance improvement of a 500-kW Francis turbine based on CFD, *Renewable Energy*, 2016, 96, 977-992.

Liu X., Luo Y., Karney B.W., Wang W., A Selected literature view of efficiency improvements in hydraulic turbines, *Renewable and Sustainable Energy Reviews* 2015, 51, 18–28.

Teegavarapu R.S.V., Simonovic S.P, Optimal operation of reservoir systems using simulated annealing, *Water Resources Management*, 2002, 16, 401-428.

Wang T., Wang C., Kong F., Gou Q., Yang S., Theoretical, experimental, and numerical study of special impeller used in turbine mode of centrifugal pump as turbine, *Energy*, 2017, accepted manuscript doi: 10.1016/j.energy.2017.04.156.

Yedidiah S., Centrifugal Pump User's Guidebook: Problem and Solutions, Chapman&Hall, 2006

Zeng Y, Liu X, Wang H. Prediction and experimental verification of vortex flow in draft tube of Francis turbine based on CFD. Procedia Engineering 2012; 31, 196-205